JACS
JOURNAL OF THE AMERICAN CHEMICAL SOCIETY

Communication

pubs.acs.org/JACS

Water Dynamics in Gyroid Phases of Self-Assembled Gemini Surfactants

Santanu Roy,*[,†] David Skoff, Dominic V. Perroni, Jagannath Mondal,[‡] Arun Yethiraj, Mahesh K. Mahanthappa,[§] Martin T. Zanni, and James L. Skinner*

Department of Chemistry, University of Wisconsin, 1101 University Avenue, Madison, Wisconsin 53706, United States

Supporting Information

ABSTRACT: Water-mediated ion transport through functional nanoporous materials depends on the dynamics of water confined within a given nanostructured morphology. Here, we investigate H-bonding dynamics of interfacial water within a "normal" (Type I) lyotropic gyroid phase formed by a gemini dicarboxylate surfactant self-assembly using a combination of 2DIR spectroscopy and molecular dynamics simulations. Experiments and simulations demonstrate that water dynamics in the normal gyroid phase is 1 order of magnitude slower than that in bulk water, due to specific interactions between water, the ionic surfactant headgroups, and counterions. Yet, the dynamics of water in the normal gyroid phase are faster than those of water confined in a reverse spherical micelle of a sulfonate surfactant, given that the water pool in the reverse micelle and the water pore in the gyroid phase have roughly the same diameters. This difference in confined water dynamics likely arises from the significantly reduced curvature-induced frustration at the convex interfaces of the normal gyroid, as compared to the concave interfaces of a reverse spherical micelle. These detailed insights into confined water dynamics may guide the future design of artificial membranes that rapidly transport protons and other ions.

Selective ion transporting materials are integral components of devices for the generation of solar fuels and for the conversion of chemical energy into electricity in fuel cells. Hydrated polymer membranes are one of the most studied classes of selective ion transporting membranes for these applications. Numerous studies have examined the structure and dynamics of water in prototypical polymer membranes such as Nafion 117, since water mediates ion transport in these materials.[1−5] Molecular dynamics (MD) simulations of these materials demonstrated that interfacial roughness of the water-filled nanochannels as well as water structure and dynamics significantly influence ion transport therein. However, the hotly debated morphologies of these nanoporous membranes have obscured direct experimental insights into how interfacial curvature of the pores influences water and ion motion.[6]

Aqueous lyotropic liquid crystals (LLCs),[7] derived from the water concentration-dependent self-assembly of amphiphiles, provide a unique platform for addressing the role of nanopore curvature on water and ion dynamics. Since LLCs comprise spatially periodic hydrophilic and hydrophobic domains with long-range nanoscale order,[8] the water within these materials is nanoconfined within monodisperse pores with well-defined curvatures. The interfacial curvature of an LLC is described either as (1) Type I or "normal", wherein the hydrophilic/hydrophobic interfaces curve toward the hydrophobic domain, or (2) Type II or "reverse" ("inverse") with opposite interfacial curvature.[9] Both normal and reverse tricontinuous network phase LLCs, such as the double gyroid (G), double diamond (D), and primitive (P) structures, are particularly useful materials in membrane applications as a consequence of their tortuous yet percolating nanochannels.[8] While network phase stability is limited in LLCs derived from single-tail amphiphiles, recent work by the groups of Gin[10,11] and Mahanthappa[12,13] demonstrate that gemini surfactants enable access to these useful lyotropic phases over wide composition and temperature phase windows.

Herein, we use a combination of two-dimensional infrared spectroscopy (2DIR)[14] and complementary MD simulations to study how interfacial curvature in a porous material affects water dynamics, by investigating the vibrational dynamics of water nanoconfined within a normal gyroid (G_I) phase. 2DIR measurements probe molecular vibrations at the nanosecond (ns) down to the femtosecond (fs) time scale, thus providing detailed information about molecular structure and stability derived from electrostatic interactions,[15] H-bonding,[16] and hydrophobicity.[17] Our studies center around an LLC G_I phase derived from the previously reported[12,18] gemini surfactant Na-74 (Figure 1a and 1b) comprising 34.4 wt % isotope-diluted water (5 mol % D_2O and 95 mol % H_2O; see Supporting Information (SI) for the sample preparation and 2DIR measurement details). This G_I LLC comprises two enantiomeric, hydrophobic networks of 3-fold connectors in a matrix of water, wherein the water is confined within convex ∼1.4 nm diameter nanochannels lined with sodium carboxylates. The composition of this LLC corresponds to a headgroup hydration number w_0 = (moles water)/(moles headgroup) = 6.5. 2DIR studies focusing on the OD stretch of isotope-diluted nanconfined water allow us to examine the influence of surfactant headgroup−water interactions on the behavior of water in the G_I phase. We also measured spectra of bulk water for comparison. All experiments were done at rt (298 K). The spectra determine OD stretch frequency correlations,[19−21] wherein the effects of strong OH couplings[22] are eliminated due to isotope dilution. Thus, only

Received: October 12, 2015
Revised: November 25, 2015
Published: February 14, 2016

DOI: 10.1021/jacs.5b12370
J. Am. Chem. Soc. 2016, 138, 2472−2475

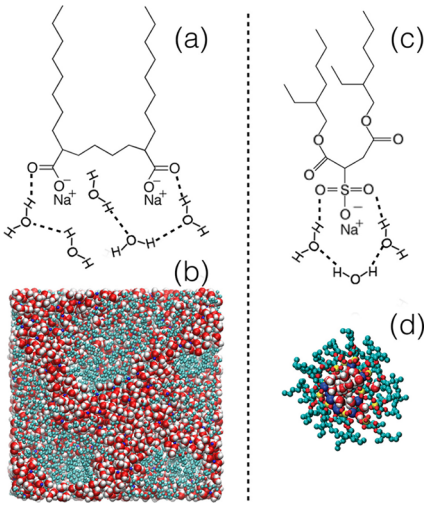

Figure 1. Molecular structure of the gemini surfactant Na-74 (a) and the AOT surfactant (c). The normal gyroid (b) and $w_0 = 2$ reverse micelle (d) structures are derived from the self-assembly of Na-74 and AOT, respectively, in the presence of water. Two major water species are identified: water H-bonded to surfactant headgroups and water H-bonded to other waters.

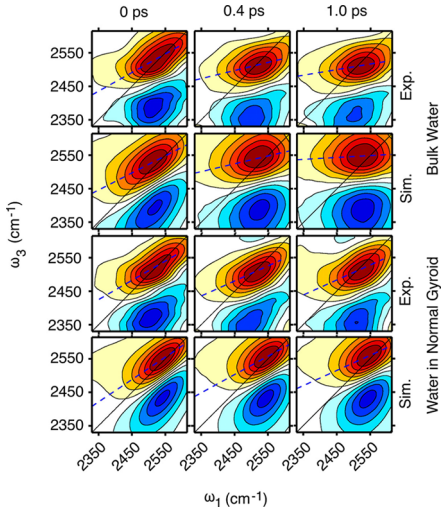

Figure 2. Experimental (Exp.) and theoretical (Sim.) 2DIR spectra for bulk water and water in the G_I phase of Na-74 gemini surfactants. These spectra correspond to the OD stretch vibration of dilute HOD in H_2O. Contours are evenly placed between −1.0 (dark blue) and 0.8 (dark red). The red peaks represent transitions between the vibrational ground and singly excited states, and the blue peaks represent transitions between the vibrational singly and doubly excited states.

local dynamical changes around OD groups are reflected in the spectra.

Interpreting experimental spectra, even for isotope-diluted water, is challenging and requires a thorough theoretical investigation. To this end, we adopt a mixed quantum-classical spectroscopic model that treats the OD chromophore quantum mechanically and all other degrees of freedom classically.[23] This model utilizes electrostatic maps[24] to extract vibrational properties such as transition frequencies and transition dipoles associated with the lowest three vibrational levels from molecular dynamics (MD) trajectories. Using these quantities and employing nonlinear response theory,[14,25] 2DIR spectra were calculated to compare with and obtain a deeper understanding of the experimental observations.

MD trajectories used here for spectral calculations were obtained in the canonical ensemble (NVT) at rt (T = 298 K) using the GROMACS package. Five independent initial configurations were chosen from a μs MD trajectory of the LLC G_I phase of Na-74 in water;[18] each was subject to time evolution for 5 ns. For the bulk water simulation, we also obtained five independent trajectories, each for 5 ns. We report the spectra that were averaged over these five trajectories. The details of MD simulations, electrostatic maps, and spectral calculations are given in the SI.

Experimental and theoretical 2DIR spectra at different t_2 for bulk and G_I-confined water are depicted in Figure 2. At $t_2 = 0$ ps, in the bulk water spectra, both experimental and theoretical 2D peaks are diagonally elongated and antidiagonally narrowed, which establishes a strong correlation between the frequencies ω_1 and ω_3. As t_2 increases, they are broadened in the antidiagonal direction and get rounder shapes, indicating loss of the frequency−frequency correlation (FFC). At t_2 = 1 ps, both experimental and theoretical spectra indicate small FFC. Yet, spectral shape changes for the G_I case are very different; differences among the spectra measured for $t_2 \leq 1$ ps are very small. All these peaks are diagonally elongated, indicating strong FFC that decays at a slower time scale. The theoretical spectra are consistent with this observation.

2DIR spectra qualitatively probe the FFC. To quantify this, we employed centerline slope (CLS) analysis.[19,20] For every ω_1, there is a ω_3 for which the diagonal peak in a 2DIR spectrum is at a maximum. The curve passing through the points corresponding to this set of ω_1 and ω_3 is the centerline. A centerline is essentially linear at the central region of a 2DIR spectrum; we did a linear least-square fit to obtain the CLS. The blue dashed lines on top of the diagonal peaks in Figure 2 are the fitted centerlines. CLS decay can be approximated as FFC decay, revealing time scales of the underlying dynamics.[19−21]

CLS decays for bulk water, obtained from analyzing both experimental and theoretical spectra, are presented in Figure 3

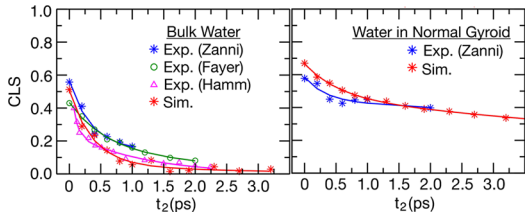

Figure 3. Centerline slope as a function of waiting time; solid lines are biexponential fits (guides to the eye). Zanni indicates our experiments, while Fayer and Hamm indicate results from refs 26 and 27, respectively.

(left panel). Experimental data for bulk water were already reported in previous studies by the Fayer[26] and Hamm[27] groups. We measured the same up to t_2 = 1 ps to reproduce their observations. We found good agreement between these experiments. Theoretical CLS decay is also consistent with the experimental ones. We observe two features in the CLS decays: an initial fast drop followed by a slower decay. These features correspond to subpicosecond (300 fs) and picosecond (1.5 ps) dynamics, respectively (the Fayer group reported these time scales from a biexponential fit to the CLS decay). In bulk water, tetrahedral geometries involving H-bonding networks can exist. Breaking and forming of these hydrogen bonds occur continuously in thermal equilibrium. Local hydrogen bond

DOI: 10.1021/jacs.5b12370
J. Am. Chem. Soc. 2016, 138, 2472−2475

fluctuations are assigned to the subpicosecond dynamics, whereas a global rearrangement of H-bonding networks is assigned to the picosecond dynamics.

Our experiments and simulations agree that the CLS decay for water in the G_I phase is much slower than that for bulk water (right panel, Figure 3). To understand this difference, we classify water hydrogens in the G_I phase into three species (Figure 1a): (a) H hydrogen-bonded to surfactant headgroups, (b) H hydrogen-bonded to other water molecules, and (c) free H (definition of H-bonding in SI). Analyzing the MD trajectories we find that the population of these species are 57%, 35%, and 8%, respectively. These species were also reported in previous studies on different surfactant−water and lipid−water interfaces by the Skinner[28−30] and Tahara[31−33] groups. They found that headgroup-bound waters are much slower than the waters bound to other water molecules. This is presumably because of the effect of the interface in disturbing bulk-water H-bonding networks, and the roughness of the interface (which increases barriers for H-bonding rearrangement). Thus, for water in the G_I phase, we find that the average dynamics of these water species, as represented by the CLS decay, is slower compared to that of bulk water.

For a given morphology, the proportion of headgroup-bound waters necessarily increases as the hydration number w_0 decreases, resulting in slower water dynamics. For example, previous experimental and theoretical studies on water inside spherical reverse micelles of AOT surfactants (Figure 1c, 1d)[30,34−37] investigated the effect of reducing w_0, thereby decreasing the size of a reverse micelle and decreasing the radius of curvature of the headgroup−water interface. Headgroup-bound waters experience increasingly more concave interfacial curvature with decreasing micelle radius and are thus geometrically constrained or jammed, leading to very slow dynamics.[30] Specifically, the idea is that for a system with high concave curvature, a nearby water molecule cannot have simultaneous favorable interactions with all of the headgroups in its proximity, and so the energy landscape becomes rougher, with higher barriers, leading to slower dynamics (compared to a flat interface). We have termed this effect "curvature-induced frustration".[30] In the case of water confined in the G_I phase, headgroup-bound waters are at a convex surface, there are no competing headgroup interactions, there is greater conformational freedom than for a flat surface, and so the dynamics should be faster.

To examine the effects of concave vs convex surfaces on water dynamics, it is interesting to compare the CLS decays for the gyroid and reverse micelle systems. To make an appropriate comparison we need to choose w_0 for the reverse micelle such that the diameter of the water pool therein is roughly the same as the diameter of the water-filled pores in the gyroid, which is about 1.4 nm, as stated earlier. Therefore, we choose $w_0 = 2$ for the reverse micelle, as shown in Figure 1d, which has a water pool diameter of about 1.6 nm.[30] We also note that in this case the fraction of water H atoms hydrogen bonded to the AOT surfactant headgroups is 42%, similar to the fraction (57%) in the gyroid phase. From consulting Figure 11 of ref 34, one can see that the experimental CLS decays more slowly for the $w_0 = 2$ reverse micelle than for the gyroid. Finally, we note that the experimental CLS decay for the gyroid extends out to only 2 ps, but we would like to make the comparison for longer times. Therefore, we focus on the theoretical CLS decays. Such calculations have previously been performed[38] for the $w_0 = 2$ reverse micelle out to 5 ps (experimental CLS results by the Fayer[34] group are in excellent agreement with these calculations; those by the Pshenichnikov[38] group are in qualitative agreement). Ideally we would like to go out to much longer times, over which structural relaxation in these systems is still going on,[30] but these results are not available to us.

In Figure 4 we show the CLS calculations for the gyroid and reverse micelle systems out to 5 ps (see SI for the corresponding

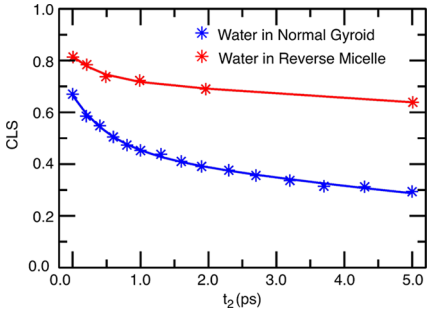

Figure 4. Theoretical centerline slope as a function of waiting time for water in the $w_0 = 2$ AOT reverse micelle[38] and in the Na-74 G_I phase. Solid lines are biexponential fits (guides to the eye).

FFC decay). The decay for the reverse micelle system is clearly slower, on both the subps and ps time scales, and there is no suggestion that this is not in fact the case on all (much longer) time scales. This is true even though the fraction of surfactant-bound water for the reverse micelle is smaller than for the gyroid. Therefore, for water pools/pores of a similar diameter and with similar fractions of surfactant-bound water, concave interfaces produce significantly slower water dynamics than convex interfaces, due to curvature-induced frustration in the former and lack of such frustration in the latter.

We acknowledge, however, that the surfactants in the two systems are not the same, and so some of the difference might be due to this, rather than to curvature. In particular, the headgroup of the gyroid surfactant is a carboxylate, while that of the reverse micelle is a sulfonate. These two headgroups have different geometries (planar versus tetrahedral, respectively), and different charges on the oxygens (−1/2 versus −1/3, respectively). The latter leads to different extents of counterion-headgroup pairing, for example. Moreover, the surfactant tails are different, and so some of the observed differences might be due to different surfactant dynamics. Nonetheless, along these lines we can make two important points. First, there is some experimental evidence[36] that the specific water−headgroup interactions are less important than the effects of confinement, per se. Second, of the effects mentioned above, we consider those due to different oxygen charges to be the most important. Here, however, the expected effect goes in the wrong direction. That is, the greater negative charge on the oxygen for the gyroid leads to stronger headgroup−water interactions, which should lead to slower water dynamics. But in fact the dynamics in the gyroid is faster, implying that the difference between the two systems is not due to the different charges.

If the ideas expressed above make sense, it stands to reason that water dynamics near flat interfaces, for example for a system with a confined water layer of about the same thickness as discussed above (1.4−1.6 nm), should be intermediate between those of the convex and concave interfaces. Although flat interfaces for the AOT surfactant system have been prepared and studied,[37] unfortunately there are no 2DIR experiments or calculations for such flat interfaces for these or similar surfactants.

DOI: 10.1021/jacs.5b12370
J. Am. Chem. Soc. 2016, 138, 2472−2475

To summarize, we have combined MD simulations with theoretical and experimental 2DIR spectroscopy to study nanoconfined water dynamics. We have found good agreement between experimental and theoretical spectra. The small discrepancies between them may arise due to not mimicking the exact experimental condition in the simulations and/or to errors in the MD and spectroscopic parameters. Nevertheless, the curvature effects on nanoconfined water dynamics have been elucidated. Water molecules can bind to lipid/surfactant headgroups of a membrane or reverse micelle through H-bonding, which affects water dynamics.[28,29,32] We have learned here that the curvature of the headgroup−water interface is an important governing factor that controls water dynamics; it is faster for convex interfaces than for concave interfaces due to more conformational freedom of waters in proximity to the convex surface.

This investigation leads to possible new directions for designing artificial membranes that can have tailored properties such as high transport rates of selected molecular or ionic species, which is possible if the membrane surfaces are convex. In the future, it will be desirable if synthetic chemists pursue experiments to design new soft energy materials with such surfaces. Experimental and theoretical 2DIR spectroscopy and MD simulations will then provide an excellent approach for examining the structure and dynamics of these new materials and their applicability in energy science.

■ ASSOCIATED CONTENT

Supporting Information

The Supporting Information is available free of charge on the ACS Publications website at DOI: 10.1021/jacs.5b12370.

Experimental details (PDF)

■ AUTHOR INFORMATION

Corresponding Authors

*E-mail: skinner@chem.wisc.edu.

*E-mail: santanu.roy@pnnl.gov.

Present Addresses

[†]Pacific Northwest National Laboratory, Richland, WA.

[‡]TIFR Centre for Interdisciplinary Sciences, Hyderabad, Telangana, India.

[§]Department of Chemical Engineering and Material Science, University of Minnesota, Minneapolis, MN.

Notes

The authors declare no competing financial interest.

■ ACKNOWLEDGMENTS

This work was primarily supported by U.S. Department of Energy (DOE) Grant No. DE-FG02-09ER16110 (S.R. and J.L.S.), and in part by U.S. DOE Grant No. DE-SC0010328 (D.V.P., A.Y., and M.K.M.), and National Science Foundation Grant CHE-0840494 (supporting the computer cluster PHOENIX at Department of Chemistry, UW-Madison, Wisconsin).

■ REFERENCES

(1) Moilanen, D. E.; Piletic, I. R.; Fayer, M. D. *J. Phys. Chem. C* **2007**, *111*, 8884.

(2) Spry, D. B.; Fayer, M. D. *J. Phys. Chem. B* **2009**, *113*, 10210.

(3) Petersen, M. K.; Hatt, A. J.; Voth, G. A. *J. Phys. Chem. B* **2008**, *112*, 7754.

(4) Jorn, R.; Savage, J.; Voth, G. A. *Acc. Chem. Res.* **2012**, *45*, 2002.

(5) Devanathan, R.; Venkatnathan, A.; Rousseau, R.; Dupuis, M.; Frigato, T.; Gu, W.; Helms, V. *J. Phys. Chem. B* **2010**, *114*, 13681.

(6) Mauritz, K. A.; Moore, R. B. *Chem. Rev.* **2004**, *104*, 4535.

(7) Kato, T.; Mizoshita, N.; Kishimoto, K. *Angew. Chem., Int. Ed.* **2006**, *45*, 38.

(8) Gin, D. L.; Bara, J. E.; Noble, R. D.; Elliott, B. J. *Macromol. Rapid Commun.* **2008**, *29*, 367.

(9) Garti, N.; Somasundaran, P.; Mezzenga, R. *Self-Assembled Supramolecular Architectures: Lyotropic Liquid Crystals*; John Wiley & Sons, Inc.: Hoboken, NJ, 2012.

(10) Pindzola, B. A.; Jin, J.; Gin, D. L. *J. Am. Chem. Soc.* **2003**, *125*, 2940.

(11) Hatakeyama, E. S.; Wiesenauer, B. R.; Gabriel, C. J.; Noble, R. D.; Gin, D. L. *Chem. Mater.* **2010**, *22*, 4525.

(12) Sorenson, G. P.; Coppage, K. L.; Mahanthappa, M. K. *J. Am. Chem. Soc.* **2011**, *133*, 14928.

(13) Sorenson, G. P.; Schmitt, A. K.; Mahanthappa, M. K. *Soft Matter* **2014**, *10*, 8229.

(14) Hamm, P.; Zanni, M. *Concepts and methods of 2D infrared spectroscopy*; Cambridge University Press: Cambridge, U.K., 2011.

(15) Volkov, V. V.; Chelli, R.; Zhuang, W.; Nuti, F.; Takaoka, Y.; Papini, A. M.; Mukamel, S.; Righini, R. *Proc. Natl. Acad. Sci. U. S. A.* **2007**, *104*, 15323.

(16) Lessing, J.; Roy, S.; Reppert, M.; Baer, M.; Marx, D.; Jansen, T. L. C.; Knoester, J.; Tokmakoff, A. *J. Am. Chem. Soc.* **2012**, *134*, 5032.

(17) Kumar, S. K. K.; Tamimi, A.; Fayer, M. D. *J. Am. Chem. Soc.* **2013**, *135*, 5118.

(18) Mondal, J.; Mahanthappa, M.; Yethiraj, A. *J. Phys. Chem. B* **2013**, *117*, 4254.

(19) Kwak, K.; Park, S.; Finkelstein, I. J.; Fayer, M. D. *J. Chem. Phys.* **2007**, *127*, 124503.

(20) Kwak, K.; Rosenfeld, D. E.; Fayer, M. D. *J. Chem. Phys.* **2008**, *128*, 204505.

(21) Roy, S.; Pshenichnikov, M. S.; Jansen, T. L. C. *J. Phys. Chem. B* **2011**, *115*, 5431.

(22) Jansen, T. L. C.; Auer, B. M.; Yang, M.; Skinner, J. L. *J. Chem. Phys.* **2010**, *132*, 224503.

(23) Skinner, J. L.; Auer, B. M.; Lin, Y.-S. *Adv. Chem. Phys.* **2009**, *142*, 59.

(24) Lin, Y.-S.; Auer, B. M.; Skinner, J. L. *J. Chem. Phys.* **2009**, *131*, 144511.

(25) Mukamel, S. *Principles of Nonlinear Optical Spectroscopy*; Oxford: New York, 1995.

(26) Park, S.; Kwak, K.; Fayer, M. D. *Laser Phys. Lett.* **2007**, *4*, 704.

(27) Perakis, F.; Hamm, P. *J. Phys. Chem. B* **2011**, *115*, 5289.

(28) Roy, S.; Gruenbaum, S. M.; Skinner, J. L. *J. Chem. Phys.* **2014**, *141*, 22D505.

(29) Gruenbaum, S. M.; Pieniazek, P. A.; Skinner, J. L. *J. Chem. Phys.* **2011**, *135*, 164506.

(30) Pieniazek, P. A.; Lin, Y.-S.; Chowdhary, J.; Ladanyi, B. M.; Skinner, J. L. *J. Phys. Chem. B* **2009**, *113*, 15017.

(31) Mondal, J. A.; Nihonyanagi, S.; Yamaguchi, S.; Tahara, T. *J. Am. Chem. Soc.* **2012**, *134*, 7842.

(32) Singh, P. C.; Nihonyanagi, S.; Yamaguchi, S.; Tahara, T. *J. Chem. Phys.* **2012**, *137*, 094706.

(33) Singh, P. C.; Nihonyanagi, S.; Yamaguchi, S.; Tahara, T. *J. Chem. Phys.* **2013**, *139*, 161101.

(34) Fenn, E. E.; Wong, D. B.; Giammanco, C. H.; Fayer, M. D. *J. Phys. Chem. B* **2011**, *115*, 11658.

(35) Tan, H.-S.; Piletic, I. R.; Riter, R. E.; Levinger, N. E.; Fayer, M. D. *Phys. Rev. Lett.* **2005**, *94*, 057405.

(36) Moilanen, D. E.; Levinger, N. E.; Spry, D. B.; Fayer, M. D. *J. Am. Chem. Soc.* **2007**, *129*, 14311.

(37) Moilanen, D. E.; Fenn, E. E.; Wong, D.; Fayer, M. D. *J. Am. Chem. Soc.* **2009**, *131*, 8318.

(38) Bakulin, A. A.; Cringus, D.; Pieniazek, P. A.; Skinner, J. L.; Jansen, T. L. C.; Pshenichnikov, M. S. *J. Phys. Chem. B* **2013**, *117*, 15545.

DOI: 10.1021/jacs.5b12370
J. Am. Chem. Soc. 2016, 138, 2472−2475